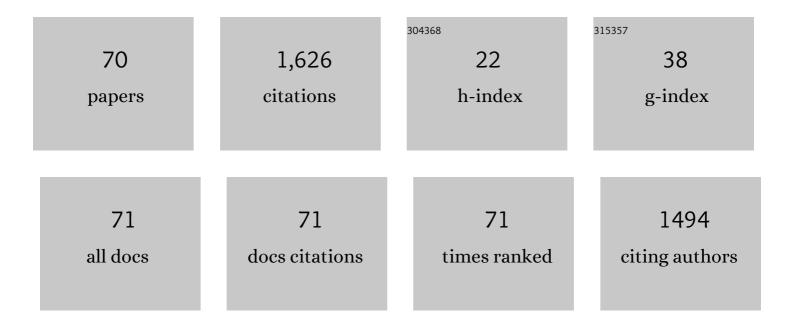
Taekyung Lee

List of Publications by Year in descending order

Source: https://exaly.com/author-pdf/3156361/publications.pdf Version: 2024-02-01



TAEKVUNG LEE

#	Article	IF	CITATIONS
1	Effects of Laser Power on the Microstructure Evolution and Mechanical Properties of Ti–6Al–4V Alloy Manufactured by Direct Energy Deposition. Metals and Materials International, 2022, 28, 197-204.	1.8	20
2	Origin of superior low-cycle fatigue resistance of an interstitial metastable high-entropy alloy. Journal of Materials Science and Technology, 2022, 115, 115-128.	5.6	10
3	Polyvinyl pyrrolidone (<scp>PVP</scp>) as an efficient and biocompatible binder for metal alloy processing: A case study with <scp>Tiâ€20Zrâ€11Nbâ€3Sn</scp> . Journal of Applied Polymer Science, 2022, 139	, 1.3	3
4	Effect on Zn on Microstructures and Mechanical Properties of Mg–Gd–Y–Zn LPSO Alloys. Metals and Materials International, 2022, 28, 2613-2620.	1.8	9
5	Tuning the texture characteristics and superelastic behaviors of Ti–Zr–Nb–Sn shape memory alloys by varying Nb content. Materials Science & Engineering A: Structural Materials: Properties, Microstructure and Processing, 2022, 845, 143243.	2.6	10
6	Manufacturing of a corrugated double-layered tube for the high-performance compact heat exchanger. International Journal of Advanced Manufacturing Technology, 2021, 112, 2065-2080.	1.5	3
7	Effect of Type-B liquid metal embrittlement cracks on high-cycle fatigue properties of spot-welded 1180 TRIP steel. Science and Technology of Welding and Joining, 2021, 26, 173-179.	1.5	2
8	Phosphorescence-Based Flexible and Transparent Optical Temperature-Sensing Skin Capable of Operating in Extreme Environments. ACS Applied Polymer Materials, 2021, 3, 2461-2469.	2.0	20
9	Accelerating globularization in additively manufactured Ti-6Al-4V by exploiting martensitic laths. Journal of Materials Research and Technology, 2021, 12, 304-315.	2.6	16
10	Effect of type-C liquid metal embrittlement on mechanical properties of spot-welded TRIP steel. Journal of Materials Research and Technology, 2021, 13, 2482-2490.	2.6	11
11	Microstructural evolution and mechanical properties of nanocrystalline Fe–Mn–Al–C steel processed by high-pressure torsion. Materials Science & Engineering A: Structural Materials: Properties, Microstructure and Processing, 2021, 827, 142073.	2.6	13
12	Effects of Substitution of Y with Yb and Ce on the Microstructures and Mechanical Properties of Mg88.5Zn5Y6.5. Metals, 2021, 11, 31.	1.0	0
13	Phosphorescence-based temperature and tactile multi-functional flexible sensing skin. Sensors and Actuators A: Physical, 2021, 332, 113205.	2.0	2
14	Accelerated recrystallization behavior of commercially pure titanium subjected to an alternating-current electropulse. Journal of Materials Research and Technology, 2021, 15, 5706-5711.	2.6	13
15	Prediction of Tempcore Rebar Strength Using a Thermomechanical Simulator with a Designed Hollow Specimen. Steel Research International, 2020, 91, 1900520.	1.0	5
16	Orientation Dependence on Plastic Flow Behavior of Hydrogen-Precharged Micropillars of High-Mn Steel. Metals and Materials International, 2020, 26, 1741-1748.	1.8	13
17	Microforming of fine metallic rods by the selective laser melting of powder. Additive Manufacturing, 2020, 36, 101612.	1.7	2
18	Microstructural Evolution of Multi-Pass Caliber-Rolled Mg–Sn and Mg–Sn–Mn Alloys. Metals, 2020, 10, 1203.	1.0	3

TAEKYUNG LEE

#	Article	IF	CITATIONS
19	Constitutive Analysis of the Anisotropic Flow Behavior of Commercially Pure Titanium. Applied Sciences (Switzerland), 2020, 10, 7962.	1.3	1
20	Graded Grain Structure to Improve Hydrogen-Embrittlement Resistance of TWIP Steel. Crystals, 2020, 10, 1045.	1.0	2
21	Microstructural Influence on Stretch Flangeability of Ferrite–Martensite Dual-Phase Steels. Crystals, 2020, 10, 1022.	1.0	8
22	Effect of undissolved Nb carbides on mechanical properties of hydrogen-precharged tempered martensitic steel. Scientific Reports, 2020, 10, 11704.	1.6	8
23	Kinetics of Capability Aging in Ti-13Nb-13Zr Alloy. Crystals, 2020, 10, 693.	1.0	7
24	Variation in Mechanical Properties of Ti-13Nb-13Zr Depending on Annealing Temperature. Applied Sciences (Switzerland), 2020, 10, 7896.	1.3	8
25	Ambivalent Role of Annealing in Tensile Properties of Step-Rolled Ti-6Al-4V with Ultrafine-Grained Structure. Metals, 2020, 10, 684.	1.0	4
26	Tailoring strength-ductility balance of caliber-rolled AZ31 Mg alloy through subsequent annealing. Journal of Magnesium and Alloys, 2020, 8, 163-171.	5.5	41
27	Breaking the limit of Young's modulus in low-cost Ti–Nb–Zr alloy for biomedical implant applications. Journal of Alloys and Compounds, 2020, 828, 154401.	2.8	38
28	Deep-learning approach to predict a severe plastic anisotropy of caliber-rolled Mg alloy. Materials Letters, 2020, 269, 127652.	1.3	6
29	Plastic anisotropy of multi-pass caliber-rolled Mg alloy with split texture distribution. Materials Science & Engineering A: Structural Materials: Properties, Microstructure and Processing, 2020, 788, 139496.	2.6	19
30	Prediction of Electropulse-Induced Nonlinear Temperature Variation of Mg Alloy Based on Machine Learning. Journal of Korean Institute of Metals and Materials, 2020, 58, 413-422.	0.4	10
31	Enhancing Superplasticity of Ultrafineâ€Grained Ti–6Al–4V without Imposing Severe Plastic Deformation. Advanced Engineering Materials, 2019, 21, 1800115.	1.6	7
32	Tempcore Process Simulator to Analyze Microstructural Evolution of Quenched and Tempered Rebar. Applied Sciences (Switzerland), 2019, 9, 2938.	1.3	10
33	Improved tensile properties of AZ31 Mg alloy subjected to various caliber-rolling strains. Journal of Magnesium and Alloys, 2019, 7, 381-387.	5.5	38
34	Sinter-joining of Cu54Zr22Ti18Ni6 BMG powder to Cu powder by spark plasma sintering. Materials Letters, 2019, 242, 55-57.	1.3	3
35	Enhanced yield symmetry and strength-ductility balance of caliber-rolled Mg–6Zn-0.5Zr with ultrafine-grained structure andÂbulk dimension. Journal of Alloys and Compounds, 2019, 803, 434-441.	2.8	22
36	Comparative study on the effects of Cr, V, and Mo carbides for hydrogen-embrittlement resistance of tempered martensitic steel. Scientific Reports, 2019, 9, 5219.	1.6	24

TAEKYUNG LEE

#	Article	IF	CITATIONS
37	High strain-rate superplasticity of AZ91 alloy achieved by rapidly solidified flaky powder metallurgy. Materials Letters, 2019, 234, 245-248.	1.3	14
38	High-Strength AZ91 Alloy Fabricated by Rapidly Solidified Flaky Powder Metallurgy and Hot Extrusion. Metals and Materials International, 2019, 25, 372-380.	1.8	22
39	Improved cold-rollability of duplex lightweight steels utilizing deformation-induced ferritic transformation. Materials Science & Engineering A: Structural Materials: Properties, Microstructure and Processing, 2019, 742, 835-841.	2.6	7
40	Prediction of hole expansion ratio for various steel sheets based on uniaxial tensile properties. Metals and Materials International, 2018, 24, 187-194.	1.8	19
41	Effects of carbon content on the tensile and fatigue properties in hydrogen-charged Fe-17Mn-xC steels: The opposing trends. Materials Science & Engineering A: Structural Materials: Properties, Microstructure and Processing, 2018, 724, 469-476.	2.6	14
42	Constitutive analysis of electrically-assisted tensile deformation of CP-Ti based on non-uniform thermal expansion, plastic softening and dynamic strain aging. International Journal of Plasticity, 2017, 94, 44-56.	4.1	50
43	Effect of the amount and temperature of prestrain on tensile and low-cycle fatigue properties of Fe-17Mn-0.5C TRIP/TWIP steel. Materials Science & Engineering A: Structural Materials: Properties, Microstructure and Processing, 2017, 696, 493-502.	2.6	24
44	Interface Characterization of Al–Cu Microlaminates Fabricated By Electrically Assisted Roll Bonding. Journal of Micro and Nano-Manufacturing, 2017, 5, .	0.8	3
45	Increased resistance to hydrogen embrittlement in high-strength steels composed of granular bainite. Materials Science & Engineering A: Structural Materials: Properties, Microstructure and Processing, 2017, 700, 473-480.	2.6	38
46	Brazing method to join a novel Cu ₅₄ Ni ₆ Zr ₂₂ Ti ₁₈ bulk metallic glass to carbon steel. Science and Technology of Welding and Joining, 2017, 22, 714-718.	1.5	12
47	Effects of drawing strain and post-annealing conditions on microstructural evolution and tensile properties of medium- and high-carbon steels. Metals and Materials International, 2017, 23, 1176-1187.	1.8	2
48	Effects of vanadium carbides on hydrogen embrittlement of tempered martensitic steel. Metals and Materials International, 2016, 22, 364-372.	1.8	71
49	Effect of Al addition on low-cycle fatigue properties of hydrogen-charged high-Mn TWIP steels. Materials Science & Engineering A: Structural Materials: Properties, Microstructure and Processing, 2016, 677, 421-430.	2.6	24
50	Role of deformation twins in static recrystallization kinetics of high-purity alpha titanium. Metals and Materials International, 2016, 22, 1041-1048.	1.8	15
51	Anisotropic properties of directed energy deposition (DED)-processed Ti–6Al–4V. Journal of Manufacturing Processes, 2016, 24, 397-405.	2.8	104
52	Superior bonding properties of dissimilar steel joint produced by electroslag remelting. Metals and Materials International, 2015, 21, 1054-1060.	1.8	2
53	Tribological and corrosion behaviors of warm- and hot-rolled Ti-13Nb-13Zr alloys in simulated body fluid conditions. International Journal of Nanomedicine, 2015, 10 Suppl 1, 207.	3.3	6
54	Manufacturing Ultrafine-Grained Ti-6Al-4V Bulk Rod Using Multi-Pass Caliber-Rolling. Metals, 2015, 5, 777-789.	1.0	24

TAEKYUNG LEE

#	Article	IF	CITATIONS
55	Role of Cu on hydrogen embrittlement behavior inÂFe–Mn–C–Cu TWIP steel. International Journal of Hydrogen Energy, 2015, 40, 7409-7419.	3.8	45
56	Phase transformation and its effect on mechanical characteristics in warm-deformed Ti-29Nb-13Ta-4.6Zr alloy. Metals and Materials International, 2015, 21, 202-207.	1.8	15
57	Surface Modification of Multipass Caliber-Rolled Ti Alloy with Dexamethasone-Loaded Graphene for Dental Applications. ACS Applied Materials & Interfaces, 2015, 7, 9598-9607.	4.0	82
58	Microstructural evolution and strain-hardening behavior of multi-pass caliber-rolled Ti–13Nb–13Zr. Materials Science & Engineering A: Structural Materials: Properties, Microstructure and Processing, 2015, 648, 359-366.	2.6	31
59	Role of Mo/V carbides in hydrogen embrittlement of tempered martensitic steel. Corrosion Reviews, 2015, 33, 433-441.	1.0	34
60	Integrated constitutive model for flow behavior of pure Titanium considering interstitial solute concentration. Metals and Materials International, 2014, 20, 1017-1025.	1.8	6
61	xmlns:mml="http://www.w3.org/1998/Math/MathML" altimg="si0002.gif" overflow="scroll"> <mml:mn>10</mml:mn> <mml:mover accent="true"><mml:mn>1</mml:mn><mml:mo>Â⁻</mml:mo><mml:mn>2</mml:mn>twins. Materials Science &: Engineering A: Structural Materials: Properties. Microstructure and</mml:mover 	>}.6	20
62	Processing, 2014, 619, 328-333. Space-holder effect on designing pore structure and determining mechanical properties in porous titanium. Materials & Design, 2014, 57, 712-718.	5.1	64
63	Effects of Tungsten Addition on the Microstructure and Mechanical Properties of Microalloyed Forging Steels. Metallurgical and Materials Transactions A: Physical Metallurgy and Materials Science, 2013, 44, 3511-3523.	1.1	12
64	Microstructure tailoring to enhance strength and ductility in Ti–13Nb–13Zr for biomedical applications. Scripta Materialia, 2013, 69, 785-788.	2.6	45
65	Internal-variable analysis of high-temperature deformation behavior of Ti–6Al–4V: A comparative study of the strain-rate-jump and load-relaxation tests. Materials Science & Engineering A: Structural Materials: Properties, Microstructure and Processing, 2013, 562, 180-189.	2.6	19
66	Grain refinement effect on cryogenic tensile ductility in a Fe–Mn–C twinning-induced plasticity steel. Materials & Design, 2013, 49, 234-241.	5.1	61
67	Mechanisms of tensile improvement in caliber-rolled high-carbon steel. Metals and Materials International, 2012, 18, 391-396.	1.8	15
68	Tensile deformation behavior of Fe–Mn–C TWIP steel with ultrafine elongated grain structure. Materials Letters, 2012, 75, 169-171.	1.3	69
69	Enhancing tensile properties of ultrafine-grained medium-carbon steel utilizing fine carbides. Materials Science & Engineering A: Structural Materials: Properties, Microstructure and Processing, 2011, 528, 6558-6564.	2.6	59
70	Work hardening associated with É≻martensitic transformation, deformation twinning and dynamic strain aging in Fe–17Mn–0.6C and Fe–17Mn–0.8C TWIP steels. Materials Science & Structured Materials Properties, Microstructure and Processing, 2011, 528, 7210, 7216	2.6	185